Crystallization and Melting Behavior of HDPE in HDPE/Teak Wood Flour Composites and Their Correlation with Mechanical Properties

Kamini Sewda, S. N. Maiti

Centre for Polymer Science and Engineering, Indian Institute of Technology, New Delhi, India

Received 8 August 2008; accepted 9 April 2009
DOI 10.1002/app.30551
Published online 22 June 2010 in Wiley InterScience (www.interscience.wiley.com).

ABSTRACT: The nonisothermal crystallization behavior and melting characteristics of high-density polyethylene (HDPE) in HDPE/teak wood flour (TWF) composites have been studied by differential scanning calorimetry (DSC) and wide angle X-ray diffraction (WAXD) methods. Composite formulations of HDPE/TWF were prepared by varying the volume fraction (Φ_f) of TWF (filler) from 0 to 0.32. Various crystallization parameters evaluated from the DSC exotherms were used to study the nonisothermal crystallization behavior. The melting temperature (T_m) and crystallization temperature (T_p) of the composites were slightly higher than those of the neat HDPE. The enthalpy of melting and crystallization (%) decrease with increase in the filler content. Because the nonpolar polymer HDPE and polar TWF are incompatible, to enhance the phase interaction maleic anhydride grafted HDPE (HDPE-g-MAH) was used as a coupling agent. A shift in the crystallization and melting peak temperatures toward the higher temperature side and broadening of the crystallization peak (increased crystallite size distribution) were observed whereas crystallinity of HDPE declines with increase in Φ_f in both DSC and WAXD. Linear correlations were obtained between crystallization parameters and tensile and impact strength. © 2010 Wiley Periodicals, Inc. J Appl Polym Sci 118: 2264–2275, 2010

Key words: high-density polyethylene; non- isothermal; crystallinity; phase interaction; melting

INTRODUCTION

Since the last three decades, efforts have been made in the direction of wood plastic composites (WPC) using commodity plastics as matrices like polyethylene (PE),[1,2] polypropylene (PP), polyvinyl chloride[3] (PVC), and polystyrene[4] (PS). High-density polyethylene (HDPE) is one of the most commonly used polyolefin with wide range of properties such as low density, good chemical resistance, good processability, toughness and flexibility, and low cost.[5] In recent years, attention has been drawn from traditional inorganic/mineral fillers (calcium carbonate, talc, calcium silicate, etc.) to biobased (wood based) fillers like wood flour, saw dust, bark flour, etc. for use in polymer composites.[6–9] Advantages offered by organic fillers over inorganic fillers are low volume cost, moderate enhancement in mechanical properties, lower specific gravity (lighter composites), reduced abrasion of processing machines, renewable in nature resulting composites recyclable.[7,8] However, HDPE is incompatible with wood flour. HDPE is a nonpolar, hydrophobic polyolefin whereas wood flour contains H—O—, Me—O— groups in cellulose, hemicellulose, and lignin units due to which it is hydrophilic and polar.[10,11] To overcome this incompatibility, various coupling agents were used which contain two functionalities, both polar and non polar, in their chemical structure which enable interaction with both HDPE and wood flour. A coupling agent enhances the interfacial adhesion at the interface by bonding or bridging at the polymer wood flour interface. Coupling agents like maleic anhydride (MAH), organosilanes, isocyanates, alkenyl succinic anhydride, stearic acid, alkyl ketene dimer, *m*-phenylenedimaleimide, and triazine derivatives have been used in WPC.[12–14] Maleic anhydride grafted HDPE (HDPE-g-MAH) has been used as a coupling agent in HDPE/wood flour composites, which contain both hydrophilic and hydrophobic moieties. The MAH group of HDPE-g-MAH may react with the hydroxyls group of wood flour whereas the HDPE component entangles with the matrix.

Because HDPE in general possesses less branching in its structure, it is a semicrystalline polymer and its crystalline morphology is responsible for its mechanical properties. Addition of fillers, coupling agents, crosslinking agents and exposure to radiation, temperature, or other agencies may disturb the crystal structure and change its material properties.[5,15,16] Extensive studies have been carried out to

Correspondence to: S. N. Maiti (maiti@polymers.iitd.ernet.in).

Contract grant sponsor: Council of Scientific & Industrial Research (CSIR).

understand the crystallization and melting behavior of HDPE in the presence of foreign or filler particles.[17,18] When cooling from the melt thermoplastic polymers generally nucleate at the surface of heterogeneities or filler loaded and a type of distorted spherulite with high density, called transcrystallinity, forms at the interface region.[17,19] Addition of any foreign particles to matrix significantly influences the degree of crystallinity, size, distribution of the crystallites, and spherulites which ultimately affect the properties of composites.[20] If the filler particles act as nucleating agents, then nucleation may give rise to reduced crystallite size, which significantly influences the properties.[20,21] In the presence of filler particles, spherulite formation can take place from the nucleus (heterogeneous nucleation) or due to temperature fluctuation in the melt (homogeneous nucleation).[16] The spherulite growth may be interrupted due to large amount of filler particles, which result into disordered structure and amorphous regions. Fillers can facilitate the crystallization of polymer matrix, which in turn can change its morphology.[20,22] It is well known that the melting range is broad for polymers, as polymer molecular chains crystallize in a wide range of sizes and with different degrees of perfections. There may be mutual interference between the molecular chains in the melt, same molecular chain passing through the crystalline, interlamellar, and amorphous regions. In polymer composites, the molecular mobility is severely constrained by the presence of any foreign inclusions.[22–24] It is well known that the addition of even small traces of foreign material to the matrix makes a considerable deviation in the crystallization temperature, spherulite size, and also have high influence on mechanical properties.[25,26]

In the present study, the crystallization and melting behavior of HDPE containing teak (*Tectona grandis*) wood flour (TWF) in the HDPE matrix are reported. Various crystallization parameters were evaluated from the exothermic peak for crystallization and analyzed on the basis of TWF concentration in the HDPE/TWF composites. Crystallinity evaluated from differential scanning calorimetry (DSC) and wide angle X-ray diffraction (WAXD) as well as crystallization parameters have been compared and correlated with the mechanical properties. Effect of a coupling agent on the crystallization and melting behavior of HDPE have also been studied and compared with HDPE/TWF composites.

EXPERIMENTAL

Materials

Injection molding grade HDPE (G-Lex I58A180), density 0.95 g cm^{-3}, MFI 18 g/10 min (230°C/ 2.16 kg) was received from the Gas Authority of India Ltd. (GAIL, Delhi, India) and used as the matrix.[27] TWF from sawdust (waste) was sieved and particles with mesh size below 180 μm with density 1.002 g cm^{-3} was used as the filler. HDPE-g-MAH, OPTIM TP-506/E (density 0.954 g cm^{-3}, MFI = 1.24 g/10 min at 230°C and 2.16 kg load, MAH content [%] 0.99, acid number 11) was obtained from Pluss Polymers Pvt. Ltd., India and used.[28] The coupling agent content was 5 wt % of the filler.

Melt blending and molding

HDPE was dry blended with the vaccum dried TWF. Composites of HDPE and TWF were prepared with volume fraction, (Φ_f), of TWF varying from 0 to 0.32 by melt compounding in a corotating twin screw extruder, Model JSW J75E IV-P (L/D = 36; diameter D = 30 mm) at a screw speed of 174 rpm. The temperature from the feed zone to the die zone was 140–180°C.[11,29] The extruded strands were pelletized. The pellets were air dried for 3 h at 60°C followed by vacuum drying at 65°C for 4 h and were injection molded into test specimens on an L&T-Demag injection molding machine (Model PFY 40-LNC 4P). The temperature ranges from the feed zone to the nozzle were 150−180°C whereas the mold temperature was 30°C. HDPE was also extruded and molded under identical processing conditions to maintain similar thermal and shear history to that of the composites.

Measurements

The crystallization studies were performed by the following two methods:

DSC measurements were performed on a Perkin Elmer Pyris-7 calorimeter, under continuous nitrogen flow of 20 mL/min. The instrument was calibrated using an indium standard (T_m = 156.4°C and ΔH = 28.4 J/g). The samples prepared for crystallization study were first filed from the injection molded tensile samples at three different regions. Powdered samples were predried for an hour at 60°C. The samples 5 mg were first heated from 30°C to 150°C, kept at 150°C for 5 min to remove the effect of previous thermal, mechanical, processing, crystallization, and shear history. The melt was then cooled down to 30°C at the rate of 10°C min^{-1} and the resulting cooling curves or exotherms were recorded. Again the samples were heated from 30°C to 150°C at the same heating rate to record the second melting curves. The second heating scans are used to determine the crystalline melting enthalpy of the matrix. The exothermic and endothermic curves were used to

study crystallization and melting characteristics of the HDPE matrix, respectively.

Crystallization and melting behaviour

The crystallization and melting studies were carried out from the exothermic and endothermic curves, respectively, which result from the increase or decrease in the enthalpy of the samples due to the presence of TWF particles.

Nonisothermal crystallization

In the DSC studies, the crystallization or the cooling curve obtained as an exothermic peak characterizes the enthalpy change during the cooling cycle. The sample was in molten state or in amorphous state at higher temperature, which gets transformed into a solid crystalline state during the cooling cycle. The crystallization parameters were evaluated from the exothermic peak to study the crystallization behavior of the composites.[25,26,30] A schematic representation of the parameters evaluated from the DSC cooling curve is shown in Figure 1. The following parameters, also described elsewhere,[25,26,30] were determined from the exotherm:

a. T_{onset}: it is the onset temperature that measures the first detectable deviation from the baseline and it indicates the initiation of crystallization.
b. T_c: it is the constructed temperature, obtained from the intercept of the tangent with the baseline toward the higher temperature side of the exotherm. This indicates the starting of crystallization process which depends on the nucleation rate.
c. T_p: this is the crystallization peak temperature, which is the intercept of the tangents drawn to both the sides of the exothermic curve, which in turn measures the temperature at the maximum crystallization rate. It is the measure of supercooling and is a function of cooling rate. Increase in nucleation rate by a nucleating agent or by some other means, results an increased T_p, i.e., decrease in supercooling.[25,30–32] Higher the peak temperature, the higher the reduction in the matrix supercooling which means more efficient is the nucleating agent.
d. $T_c - T_p$: it is a measure of the crystal growth rate, lower the value, higher the crystal growth rate, i.e., the higher the rate of crystallization, smaller the difference between the temperatures.
e. S_i: it is the initial slope in the higher temperature side of the cooling curve, which is measured from the tangent of an angle formed by the upward surge of the curve; it is a measure of the nucleation rate for crystallization.
f. ΔW: it is the width of the curve at half height and is a measure of crystallite size distribution; higher the value, broader the distribution.
g. A/m (Area/mass): this is the ratio of the curve for crystallizable component of the composite, and is a direct measure the degree of crystallinity. The heat of fusion and crystallization are directly related to the amount of crystalline phase. The higher the value the higher the ease of crystallization also.

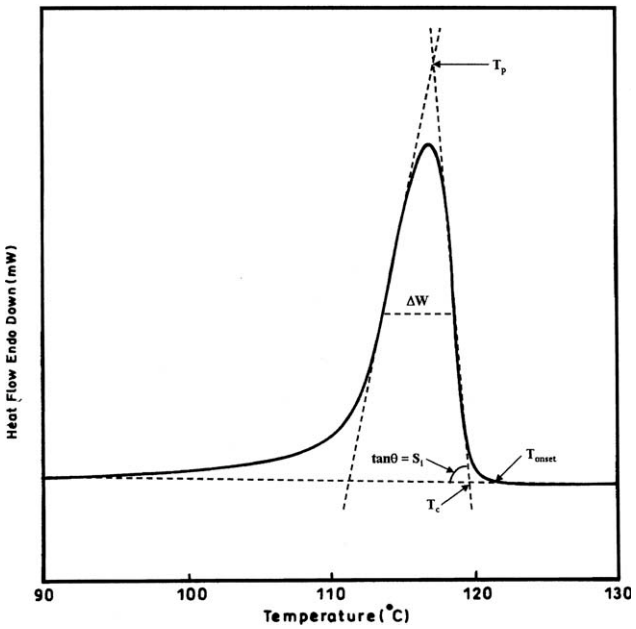

Figure 1 Schematic representation of the parameters evaluated from crystallization exotherm for HDPE.

These parameters give an insight into the morphology of the crystalline phase. It can be seen that if there is a decrease in S_i it may be followed by an increase in ΔW. Slower nucleation rate results in the delayed crystallite formation.[26,30,33] If a filler facilitates the nucleation, the result is an increased number of crystallites with reduced size in the composite. T_c increases with increase in the nucleation effect of a filler.[20]

Melting

1. In the DSC scans, the second heating curve obtained as an endothermic peak results from the melting of solid, crystalline state to molten amorphous state which follows the endothermic enthalpy change, Figure 2. The heat of fusion was used to evaluate the degree of crystallinity (%) following eq. (1) for normalized sample of

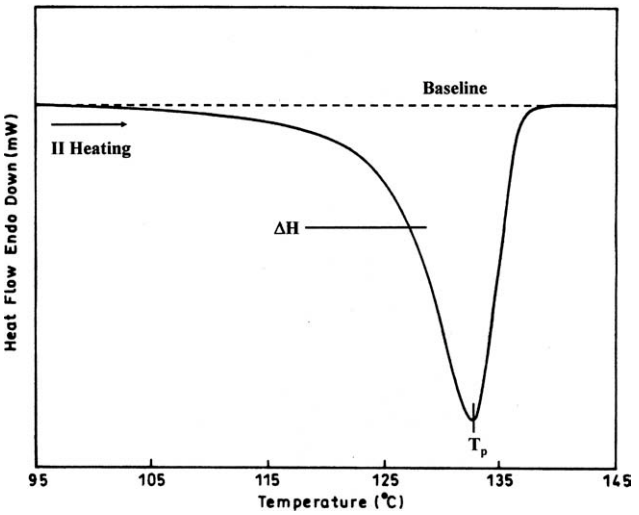

Figure 2 Schematic representation of melting endotherm for HDPE.

5 mg while considering the enthalpy for 100% crystalline PE, ($\Delta H_{\text{theoretical}} = 277\text{J/g}$)[34]:

$$\text{Degree of crystallinity} = [(\Delta H_{\text{experimental}}/W_{\text{HDPE}}) /\Delta H_{\text{theoretical}}] \times 100 \quad (1)$$

where W_{HDPE} is weight fraction of HDPE in the composites.

2. The wide angle X-ray diffraction (WAXD) studies were carried out on Philips WAXD machine (PANalytical diffractometer) in the angular range of $2\theta = 10$–35°. The degree of crystallinity was calculated from the WAXD data by following the eq. (2), (using simple peak area method):[15]

$$\text{Degree of crystallinity, } X_c(\%) = [A_{\text{cr}}/(A_{\text{cr}}/A_{\text{am}})] \times 100 \quad (2)$$

where A_{cr} = scattering from the crystalline regions; A_{am} = amorphous scattering; $A_{\text{am}} + A_{\text{cr}}$ = total sample scattering.

Evaluation of mechanical properties

Tensile and impact tests have been performed according to the ASTM D638, ASTM D256 test methods, respectively.[35] Tensile properties were measured on a Zwick Universal Tester, Model Z010, at a cross-head speed 100 mm/min and cross-head separation 60 mm. The notched Izod impact measurements were performed on a falling hammer type Atsfaar Charpy Impact tester, Model Impacts–15. Average value of six samples was reported for each composite composition. All measurements were carried out at ambient temperature, 30 ± 2°C.

RESULTS AND DISCUSSION

Crystallization and melting behaviour

Nonisothermal crystallization

The DSC scan of TWF which does not show any crystallization or melting peak indicating that there was no crystallizable component in the TWF under the conditions of DSC measurements. The HDPE shows the crystallization and melting peak in the range of 110–120°C and 130–135°C, respectively Figure 3, depends on the rate of cooling, heating, molecular weight, and additives.[36–38] The addition of TWF to HDPE decreases the total enthalpy of crystallization of neat HDPE, the maximum energy liberated during crystallization process of neat HDPE.[37] In the absence of any foreign particles, there was no hindrance to the nucleation (self-nucleation) and growth of crystallites was rapid, thus large amount of heat liberated during the process. Crystallization exotherm peak in the DSC scan was obtained predominantly during the cooling cycle, a single well-defined exothermic peak was observed, corresponding to HDPE at 117.1°C, Figure 3. It is obvious that the nonisothermal crystallization behavior of HDPE is altered significantly with the incorporation of TWF. For the HDPE/TWF composite systems, the exothermic peak becomes wider with no change in T_p with the increase in Φ_f, Figure 3.

Although for the HDPE/TWF/HDPE-g-MAH systems the peak temperature shifted toward higher temperatures with increase in Φ_f, which indicates that, the crystallization starts at higher temperature, due possibly, to the nucleating effect of TWF in presence of the coupling agent, Figure 4. The peak widens with increase in Φ_f, which indicates wide distribution of the crystallite size. The curve also becomes steeper toward the higher temperature side

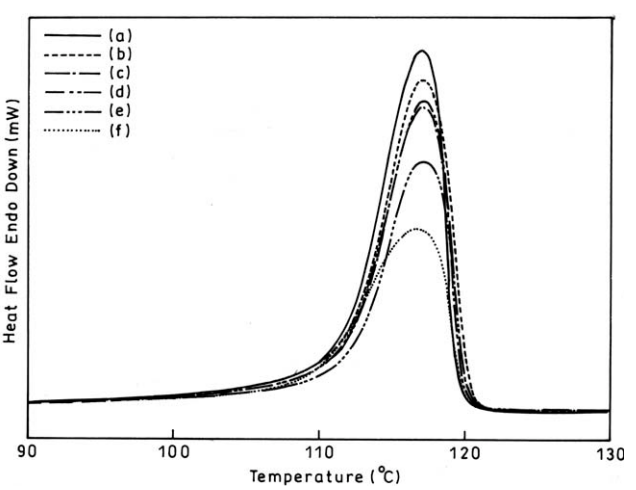

Figure 3 Crystallization exotherms for the HDPE/TWF composites at varying Φ_f: (a) 0.00, (b) 0.05, (c) 0.09, (d) 0.16, (e) 0.25, and (f) 0.32.

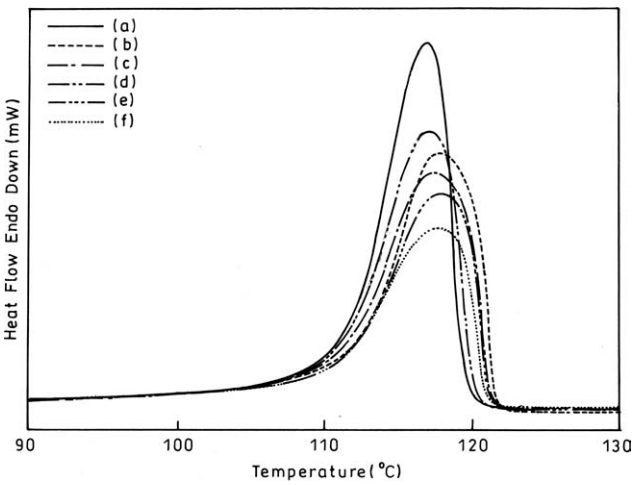

Figure 4 Crystallization exotherms for the HDPE/TWF/HDPE-g-MAH composites at varying Φ_f: (a) 0.00, (b) 0.05, (c) 0.09, (d) 0.16, (e) 0.25, and (f) 0.32.

with increase in Φ_f, which means fast crystallization due to the presence of the TWF on addition of the coupling agent. TWF particles act as efficient nucleating agent and facilitate the crystallization of HDPE in the HDPE/TWF/HDPE-g-MAH systems. HDPE-g-MAH greatly influences the composite morphology, which in turn influences the shape and position of the crystallization exotherm, as the maximum crystallization temperature (T_p) increased.[39]

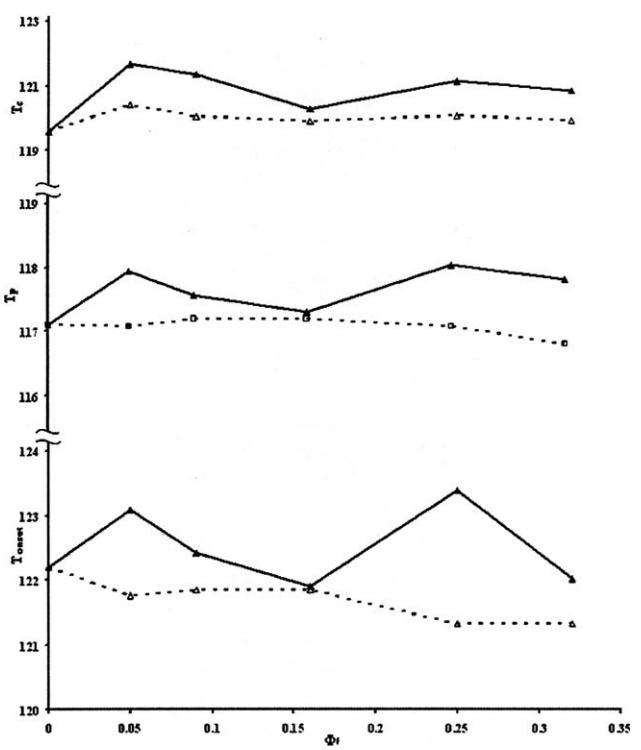

Figure 5 Variations of parameters T_{onset}, T_p, and T_c as a function of Φ_f for the HDPE/TWF (□----) and the HDPE/TWF/HDPE-g-MAH (▲—) composites.

The parameters T_{onset}, T_c, T_p, $T_c - T_p$, S_i, ΔW, and A/m demonstrate nonlinear variations. The variations of these parameters with Φ_f were divided into three distinct regions of compositions for the HDPE/TWF and the HDPE/TWF/HDPE-g-MAH composite systems as follows, (Figures 5, 6 and Table I):

a. Low TWF content, $\Phi_f = 0$ to 0.05,
b. moderate TWF content, $\Phi_f = 0.05$ to 0.16,
c. high TWF content, $\Phi_f = 0.16$ to 0.32.

In the region (a) of the HDPE/TWF composite composition, incorporation of TWF results in decreased T_{onset}, T_p, S_i, and A/m whereas T_c, $T_c - T_p$, and ΔW increased. On account of lower rate of nucleation (decreased S_i), a small number of spherulite will result and the spherulite will grow in larger size, as TWF content is low despite the fact that some spherulite may also be smaller in size due to slow crystallization growth rate (higher $T_c - T_p$) and

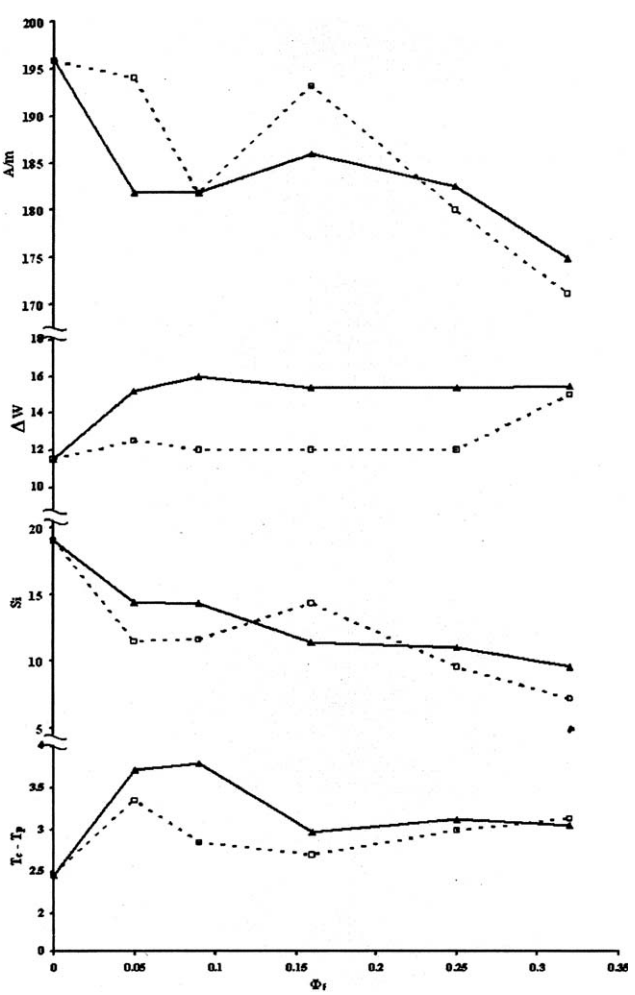

Figure 6 Variations of parameters $T_c - T_p$, S_i, ΔW and A/m, as a function of Φ_f for the HDPE/TWF (□----) and the HDPE/TWF/HDPE-g-MAH (▲—) composites.

TABLE I
Crystallization Parameters Obtained from the DSC Cooling Curves of HDPE, HDPE/TWF, and HDPE/TWF-HDPE-g-MAH (in Parentheses) Composites

Φ_f	T_p (°C)	T_c (°C)	ΔW (Arb. unit)	T_{onset} (°C)	$T_c - T_p$ (°C)	A/m (Arb. unit)	S_i (Arb. unit)
0	117.1	119.6	11.5	122.2	2.5	195.9	19.1
0.05	117.1 (117.9)	120.4 (121.7)	12.5 (15.2)	121.8 (123.1)	3.4 (3.7)	194.1 (181.8)	11.4 (14.4)
0.09	117.2 (117.6)	120.0 (121.4)	12.0 (16.0)	121.9 (122.4)	2.9 (3.8)	181.8 (181.8)	11.6 (14.3)
0.16	117.2 (117.3)	119.9 (120.3)	12.0 (15.4)	121.9 (121.9)	2.7 (3.0)	193.2 (185.9)	14.3 (11.4)
0.25	117.1 (118.0)	120.1 (121.1)	12.0 (15.4)	121.3 (123.4)	3.0 (3.1)	180.0 (182.5)	9.5 (11.0)
0.32	116.8 (117.8)	119.9 (120.9)	15.0 (15.5)	121.3 (122.0)	3.1 (3.1)	171.2 (174.9)	7.2 (9.5)

disturbance created by the TWF particles. Thus, decrease in the degree of crystallinity (decreased A/m) and a slight increase in the crystallite size distribution parameter (ΔW) in this region of TWF concentration are in agreement with this morphological description of HDPE in the composites, Figures 3, 5, and 6 and Table I.

In the region (a) of the HDPE/TWF/HDPE-g-MAH composites, addition of the coupling agent, HDPE-g-MAH, leads to decrease in the nucleation rate of crystallization (decrease in S_i) and lower the rate of crystallization growth rate (higher $T_c - T_p$) than the HDPE/TWF composites, Figures 4, 5, and 6 and Table I. The coupling agent increases the phase interaction and adhesion between HDPE and TWF. HDPE-g-MAH acts as a bridging agent between the phases. This interaction and bridging interferes with the nucleating effect of TWF although a surface may be provided for heterogeneous crystallization which would lead to the decreased rate of crystal nucleation and growth rate of crystallization. Because of this obstruction, the spherulites formed would be relatively less in number but few of the spherulites may not grow to optimum size and will remain small, this will leads to broader distribution of crystallites which was indicated by the increase in crystallization distribution parameter ΔW. Although early crystallization is initiated, lack of nucleation and slow growth rate gives low degree of crystallinity also which is in good agreement with the morphological description of HDPE in the composites with the coupling agent.

The degree of crystallinity values were higher for HDPE/TWF composites. The coupling agent in the system binds the phases by chemical bond and physical interaction.[11,40] For crystallization, HDPE is less free in the system. The mobility of HDPE chains is restricted by the coupling agent. So only few crystals or spherulites may form which gives rise to decreased degree of crystallinity (lower value A/m). The crystallization exotherm peak temperature (T_p) shows higher values which indicates that the peak shifts toward higher temperature side and the crystallization facilitated in the presence of coupling agent due to enhanced wetting of TWF by the coupling agent, as compared to the HDPE/TWF composite systems.

In the region (b) of the HDPE/TWF composite, slight increase in the nucleation rate of crystallization (increase in S_i) was observed whereas crystal growth rate (increased $T_c - T_p$) decreased; however, the degree of crystallinity (A/m) increased after initial decrease with increasing TWF concentration. The spherulites will be of smaller and of almost equal size because of generation of relatively large number of spherulite sites. A very small decrease and then almost constant value for ΔW in this region, implies relatively narrower distribution of spherulites which in turn results in the increase in the degree of crystallinity (A/m), which supports this morphological explanation of the HDPE in HDPE/TWF composites, Figures 3, 5, and 6 and Table I.

On the other hand for the HDPE/TWF/HDPE-g-MAH composite, in the region (b) the nucleation rate of crystallization (S_i) decreases whereas crystal growth rate increases ($T_c - T_p$ decreases) (Figs. 4, 5, 6; Table I). Because of small number of nucleating sites for spherulite formation and increased rate of crystallization, spherulites grow faster but all spherulites may not find enough space and orientation to grow bigger due to the bridging introduced by the coupling agent. This gives rise to slightly increased ΔW (broader crystal size distribution), which would remain constant. ΔW values for the HDPE/TWF composites were lower than the HDPE/TWF/HDPE-g-MAH systems throughout the TWF concentration. The overall rate of crystallization was higher in the HDPE/TWF system leading to slight increase in the degree of crystallinity (A/m). The degree of crystallinity inappreciably increases for the HDPE/TWF/HDPE-g-MAH, remaining, however, lower than the neat HDPE and corresponding HDPE/TWF composite system. T_{onset} and T_p decrease in this region but the values are higher than those of the corresponding HDPE/TWF composite. This also has the similar implication as decrease in the values of S_i.

In the region (c) of the HDPE/TWF composites, due to slow nucleation rate (decrease in S_i, lower than the other two regions) larger spherulite will form and because of lower crystal growth rate ($T_c - T_p$

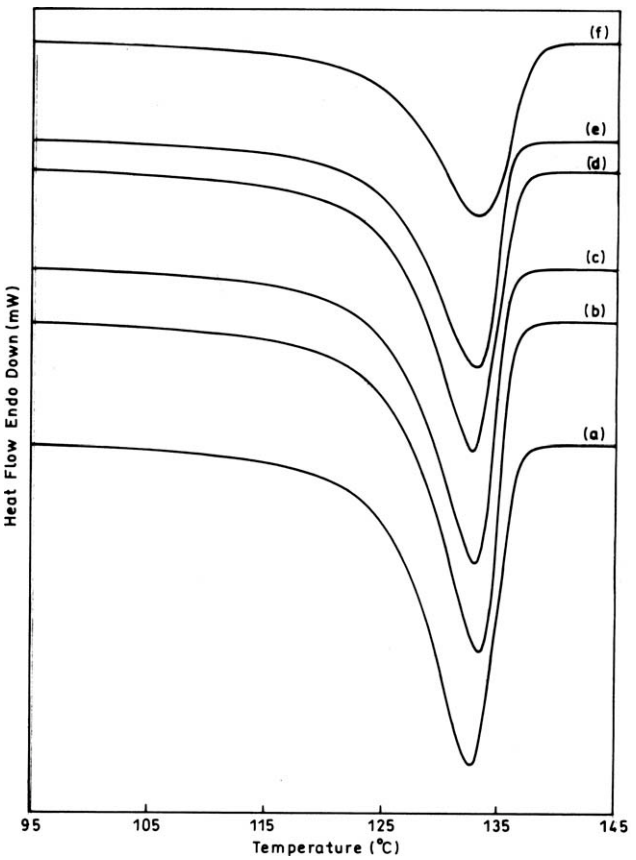

Figure 7 DSC melting endotherms for the HDPE/TWF composites at varying Φ_f: (a) 0.00, (b) 0.05, (c) 0.09, (d) 0.16, (e) 0.25, and (f) 0.32.

increases) decrease in the degree of crystallinity (A/m) will result with increase in TWF concentration, Figures 3, 5, and 6 and Table I. Spherulites formed were small in number due to slow nucleation rate and slow crystallization; crystallites grow in an uneven fashion. Thus, crystallites distribution becomes wider (ΔW increases) as small and large spherulites will coexist and will remain unchanged with further increase in Φ_f which ultimately results in the decrease in the degree of crystallinity.

For the HDPE/TWF/HDPE-g-MAH composites in the region (c) the overall rate of crystallization decreases ($T_c - T_p$ higher than the neat HDPE) marginally and the crystallite distribution parameter (ΔW) remains unchanged, Figures 4, 5, and 6 and Table I. In the presence of the coupling agent, there was good adhesion between TWF and the matrix, chain stiffness increases and the interaction between the chains may increase which prevents the formation of crystallites. The chains may not be able to arrange properly to form crystalline structure. Thus, nucleation rate of crystallization and degree of crystallinity show decreasing trend, which may explain the morphology of HDPE in the composites.

In the HDPE/TWF or the HDPE/TWF/HDPE-g-MAH systems, TWF acts as a nucleating agent which is evidenced by higher T_{onset} as compared to that of the neat HDPE. In the composites nucleation increased the number of crystalline units, like spherulite and lamellae, due to this their size reduced and distribution becomes broader.[21] The coupling agent, HDPE-g-MAH enhanced the filler matrix interaction which also helps in deagglomeration of discrete filler particles and thus improves the filler dispersion. Because of better dispersion and favorable orientation of the filler particles the initiation of crystalline units enhanced to a degree. Thus, the T_{onset}, T_c, and T_p have higher values for the HDPE/TWF/HDPE-g-MAH system as compared to the HDPE/TWF system.

Melting behaviour of HDPE in HDPE/TWF composites

The second heating endotherm obtained for the HDPE/TWF and the HDPE/TWF/HDPE-g-MAH composites were plotted in Figures 7 and 8, respectively. The melting temperature T_m, and heat of fusion or melting (ΔH_f or ΔH_m) obtained from reheating scans are presented in Table II.

The total heat of fusion (ΔH_f) decreases linearly with increase in Φ_f with regression coefficient,

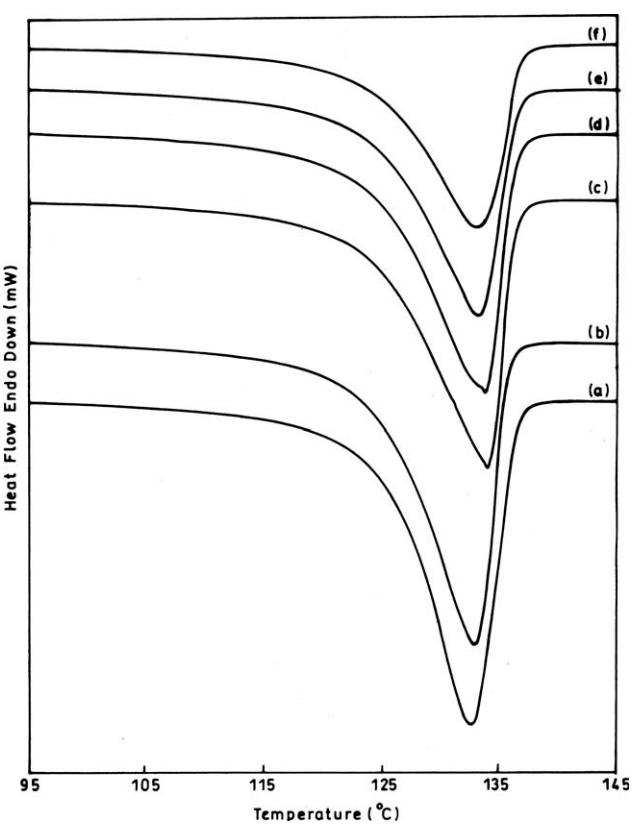

Figure 8 DSC melting endotherms for the HDPE/TWF/HDPE-g-MAH composites at varying Φ_f: (a) 0.00, (b) 0.05, (c) 0.09, (d) 0.16, (e) 0.25, and (f) 0.32.

TABLE II
Crystallization Parameters ΔH_f, T_m, and Crystallinity (%) from the Melting DSC Heating Scans of the HDPE/TWF and the HDPE/TWF/HDPE-g-MAH Composites

	HDPE/TWF			HDPE/TWF/HDPE-g-MAH		
Φ_f	ΔH_f (J/g)	T_m (°C)	Crystallinity (DSC) (%)	ΔH_f (J/g)	T_m (°C)	Crystallinity (DSC) (%)
0	180.2	132.7	65.0	180.2	132.7	65.0
0.05	165.3	133.4	62.7	158.5	133.1	61.1
0.09	153.6	132.8	61.0	153.0	134.0	60.8
0.16	142.8	132.6	61.9	138.4	133.8	60.0
0.25	123.8	133.0	60.3	117.9	133.2	57.5
0.32	108.2	132.8	58.6	105.4	132.9	57.1

$R^2 = 0.99$ and 0.98, for the HDPE/TWF and the HDPE/TWF/HDPE-g-MAH, respectively, Figure 9.

The first heating curve cannot be considered for analysis because different samples experiences different stress during processing. The melting endotherm peak was obtained predominantly during the second heating cycle, a single well-defined endothermic peak was observed, corresponding to HDPE at 132.7°C. In the HDPE/TWF composites, the breadth of the endotherm is higher in comparison to the height with increasing Φ_f. The melting endotherm decreases in size and T_m increases with increase in Φ_f, Figure 7. This is attributed to the fact that while cooling HDPE matrix melt nucleates on the surface of the TWF at relatively high temperature and forms crystal lamellas with more perfection and larger thickness, resulting high T_m.[41] ΔH_f is sensitive to structural imperfections resulting from processing, impurities, and the presence of filler. And also previous thermal history has large influence on ΔH_f. The T_m increases as the intermolecular interaction or interfacial adhesion and chain stiffness increases.[16]

The degree of crystallinity (%) calculated for the HDPE/TWF and the HDPE/TWF/HDPE-g-MAH systems from the ΔH_f followed a decreasing trend, Figure 9 and Table II. The crystallinity of HDPE decreased in the presence of the TWF particles, which provide mechanical restraints restricting the movement of HDPE polymer chains to crystallize. In the HDPE/TWF/HDPE-g-MAH composites the crystallinity were a degree lower to those of the HDPE/TWF composites at the corresponding Φ_f values, Figure 9 and Table II. The chain entanglement between HDPE and HDPE-g-MAH, and the chemical reaction between TWF and HDPE-g-MAH limit the movement of HDPE chains in the HDPE/TWF/HDPE-g-MAH systems. The decrease in the parameter indicates enhanced phase adhesion in HDPE/TWF/HDPE-g-MAH systems due to the presence of the coupling agent.

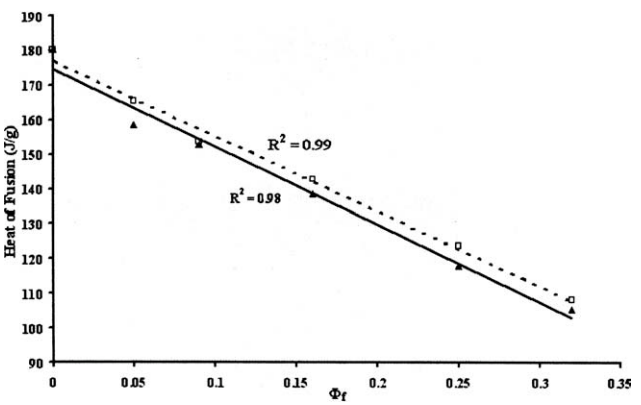

Figure 9 Variation of ΔH_f for the HDPE/TWF (□----) and the HDPE/TWF/HDPE-g-MAH (▲—) composites as a function of Φ_f.

Wide angle X-ray diffraction studies

WAXD provides direct information on the crystallinity, preferred orientation, phase identification, and composition of composites. X-ray diffractograms of HDPE and the HDPE/TWF composites, the intensity (I) – diffraction angle (2θ) variations are plotted in Figure 10. HDPE shows the diffraction pattern with two maxima at 2θ at 22.4° and 24.7° which are very intense, also observed in other works.[15,36,42,43]

In HDPE/TWF composites, these characteristic peaks of HDPE were found indicating that HDPE was the only crystallizable component in these composites. The intensity of the HDPE peak decreases with the increase in the TWF concentration, Figure 10. The HDPE peak at $2\theta = 24.7°$ was found to be well-defined sharp peak up to $\Phi_f = 0.16$, whereas the peak broadens at $\Phi_f = 0.25$ and 0.32. This shows that the spherulite size distribution becomes broader with the increase in the Φ_f and thus the results were in good agreement with the DSC studies as well.

In the HDPE/TWF/HDPE-g-MAH composites, the same pattern of the diffraction was obtained; however, the corresponding intensity of the composites were lower compared to the HDPE/TWF composites, Figure 11. This was attributed to the chemical interaction between the HDPE and the TWF through the HDPE-g-MAH, which restricts the mobility of the HDPE matrix chains.

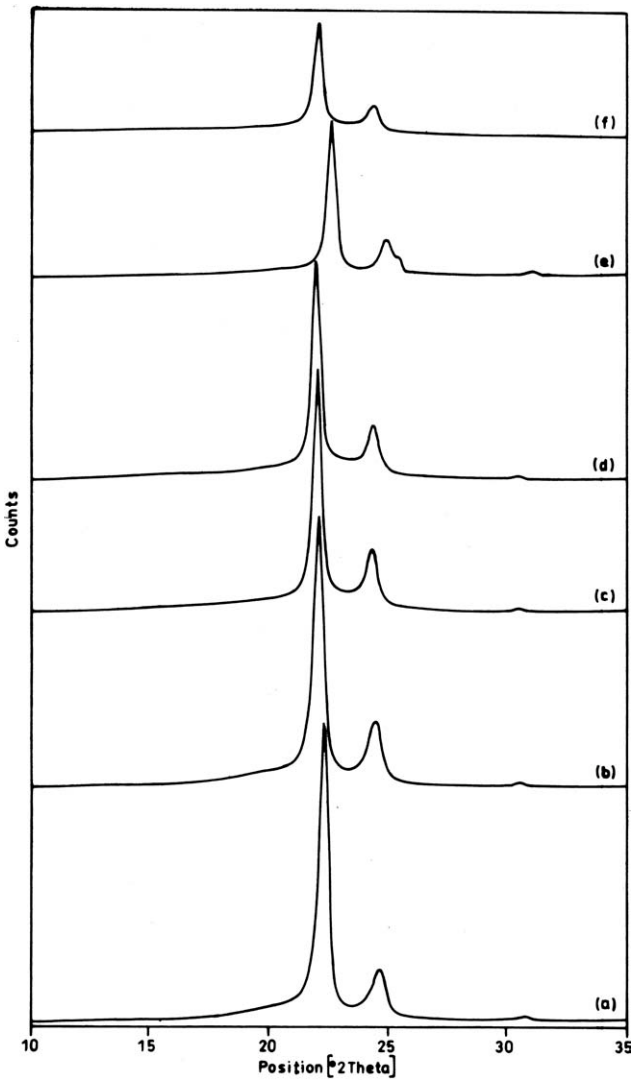

Figure 10 X-ray diffractograms of HDPE (a) and the HDPE/TWF composites at varying Φ_f: (b) 0.05, (c) 0.09, (d) 0.16, (e) 0.25, and (f) 0.32.

The degree of crystallinity (X_c) calculated from diffractograms using the method described in experimental section, decreased with increase in the Φ_f, Figure 12 which was also found in the DSC studies.

Mechanical properties

The tensile properties of the HDPE/TWF composites such as tensile strength (σ), modulus (E), and elongation-at-break (ε) (%) were plotted against Φ_f, Figure 13. In the region (a), $\Phi_f = 0$ to 0.05 of the composite composition of the HDPE/TWF system, the tensile strength and modulus increased slightly while elongation (%) and impact strength (I) decreased rapidly which may be due to increase in the stiffness and rigidity in the system.[9] Crystallinity obtained from both DSC and WAXD studies decreased in this range as in crystallization exotherm. Crystallite size distribution (ΔW) was slightly higher.

Although in the HDPE/TWF/HDPE-g-MAH composites, tensile strength and modulus show same amount of increase as that of the HDPE/TWF. On the other hand, elongation shows slightly higher values and impact strength values were lower to the HDPE/TWF composites.[9] This may be due to the presence of the coupling agent that resulted in chemical interaction between HDPE and TWF and formation of interfacial region. Because of that crystallinity decreases but the crystallite distribution parameter, ΔW, increased. The crystallization peak temperature, T_p, shifted toward higher temperature as the presence of HDPE-g-MAH facilitates the crystallization of HDPE to some extent.

In the region (b), $\Phi_f = 0.05$ to 0.16 all the properties, i.e., tensile strength and modulus, elongation, and impact strength decrease with decrease in the crystallinity of HDPE in the HDPE/TWF, Figure 13.[9] The ΔW remains constant in this region. Although in case of HDPE/TWF/HDPE-g-MAH composites, the

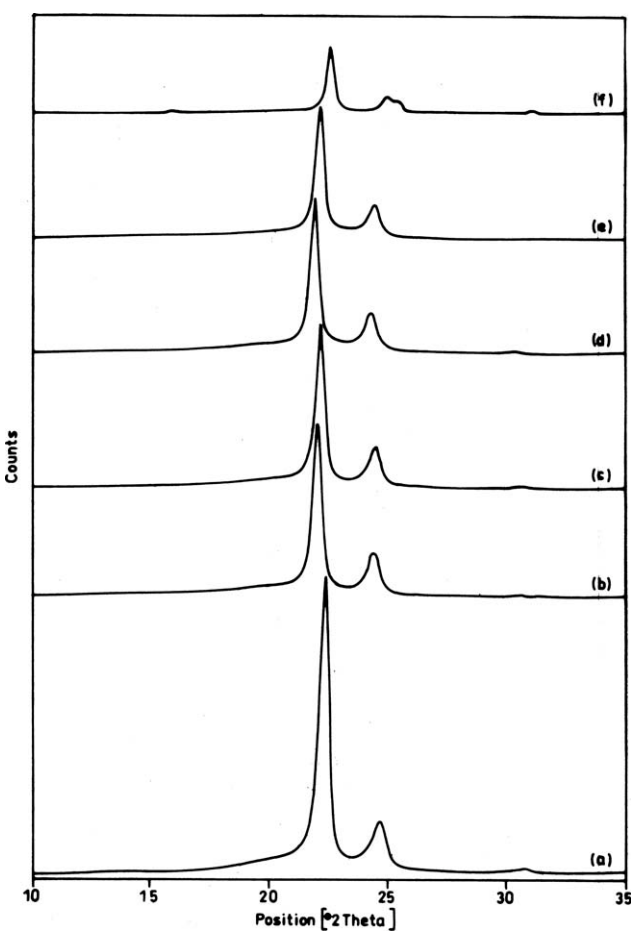

Figure 11 X-ray diffractograms of HDPE (a) and the HDPE/TWF/HDPE-g-MAH composites at varying Φ_f: (b) 0.05, (c) 0.09, (d) 0.16, (e) 0.25, and (f) 0.32.

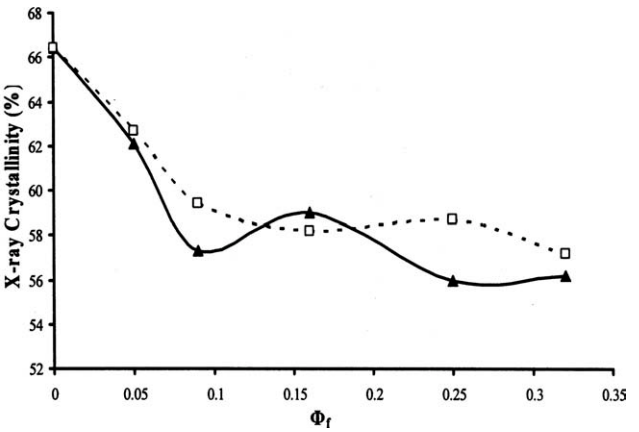

Figure 12 Variation of X-ray crystallinity with Φ_f for the HDPE/TWF (□) and the HDPE/TWF/HDPE-g-MAH (▲) composites.

tensile modulus and strength slightly decreases at $\Phi_f = 0.09$ the value then increase at $\Phi_f > 0.09$.

In the region (c), $\Phi_f = 0.16$ to 0.32 of the HDPE/TWF composites, tensile modulus and impact strength decreases more rapidly while elongation and impact strength decrease and level off with increase in the Φ_f. Crystallinity decreased and ΔW increased which imply that the distribution of crystallites becomes broader while there was hindrance in the crystallization of HDPE.

In the HDPE/TWF/HDPE-g-MAH composites, tensile strength and modulus increased with Φ_f whereas the elongation and impact strength decreased. The crystallinity shows lower values than that of HDPE/TWF composites and the shift in the crystallization exotherm toward the higher temperature was higher, i.e., the crystallization process starts at higher temperature in the presence of HDPE-g-MAH which in turn facilitates the crystallization. The parameter ΔW level off in this region.

Hence, in the presence of HDPE-g-MAH, composites show higher strength properties as the crystallinity decreased compared to that of the HDPE/TWF systems. The enhanced interaction between the HDPE and TWF was responsible for superior properties as stress transfer from HDPE to TWF was facilitated in the presence of HDPE-g-MAH due to the formation of an interface layer which was absent in case of the HDPE/TWF composites. In the HDPE/TWF, only physical interaction due to differential thermal shrinkage was present which only increases the stiffness in the system.

Correlation of crystallization parameters with mechanical properties

Systematic effects of enhanced crystallization parameters, such as nucleation rate, degree of supercooling, and the degree of crystallinity on the tensile properties of PP, were reported by Beck and Ledbetter.[32,44] Tensile strength, modulus, yield strength, and elongation-at-break showed linear variations with T_p. In PP/elastomer blends, Gupta and Purwar[26] obtained linear correlations of tensile properties with T_p and ΔW (spherulite size distribution parameter). In this work, we observed similar linear correlations of tensile properties and impact strength of the HDPE/TWF and the HDPE/TWF/HDPE-g-MAH composites with S_i, ΔH, ΔW, A/m, and X_c as presented in Table III. Regression analysis was performed to estimate the linearity of the correlations. The values of the coefficient of correlation above, $R^2 \geq 0.70$ were assumed to represent a moderate linearity of correlation in view of the data scatter in such experimental work with heterogeneous systems. The

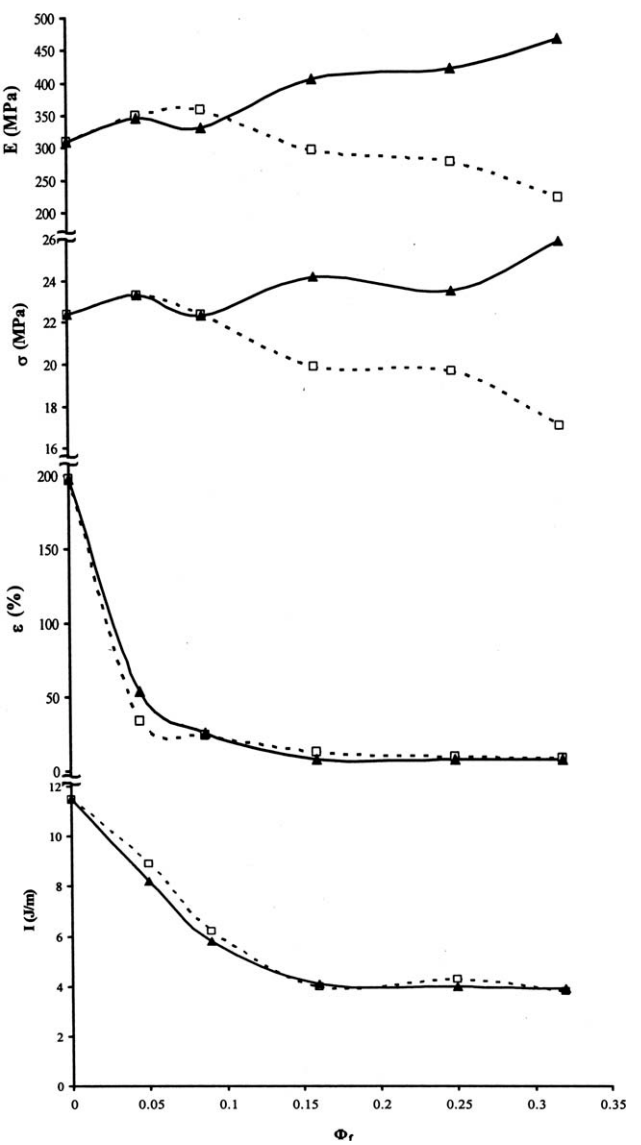

Figure 13 Plots of tensile and impact properties of the HDPE/TWF composites (□) and the HDPE/TWF/HDPE-g-MAH (▲) with Φ_f.

TABLE III
Correlation of Tensile, Impact Properties, and X-Ray Crystallinity with Crystallization Parameters

		HDPE/TWF		HDPE/TWF/HDPE-g-MAH	
Y axis	Crystallization parameter (*X* axis)	Linear equation	Correlation coefficient (R^2)	Linear equation	Correlation coefficient (R^2)
Tensile modulus (MPa)	S_i	–	–	$y = -16.627x + 601.49$	0.86
	ΔH	–	–	$y = -19.297x + 1543.4$	0.81
Elogation-at-break (%)	S_i	$y = 13.188x - 116.52$	0.71	$y = 17.485x - 187.16$	0.84
	ΔW	–	–	$y = -38.164x + 611.06$	0.93
	A/m	–	–	$y = 7.967x - 1419.3$	0.71
	ΔH	$y = 20.317x - 1179.1$	0.79	$y = 24.535x - 1466.9$	0.70
	X_c	$y = 16.943x - 979.85$	0.82	$y = 14.706x - 830.02$	0.84
Impact Strength (J/m)	S_i	–	–	$y = 0.8525x - 5.068$	0.92
	ΔW	–	–	$y = -1.5606x + 29.399$	0.71
	ΔH	$y = 1.2558x - 70.889$	0.77	$y = 0.984x - 53.033$	0.85
	X_c	$y = 0.8914x - 47.42$	0.97	$y = 0.7142x - 36.243$	0.90
X_c	S_i	–	–	$y = 1.0536x + 45.512$	0.80
	ΔW	–	–	$y = -2.1237x + 91.001$	0.75
	A/m	–	–	$y = 0.4828x - 29.231$	0.71
	ΔH	$y = 1.4507x - 28.904$	0.84	$y = 1.3108x - 19.476$	0.86

linear equations with the corresponding R^2 values are shown in Table III.

In the HDPE/TWF composites, linear correlations were obtained with ε (%) vs. S_i, ΔH, and X_c, and with I vs. ΔH and X_c, Table III, where ε (%) is the elongation-at-break (%) and I is the impact strength. Correlation of X_c and ΔH is also shown in Table III. This correlation is quite linear with $R^2 = 0.84$, which indicates good consistency between X-ray and DSC crystallinity.

In presence of the coupling agent, linear correlations between the tensile property such as ε (%) and the impact strength, I, and the crystallization parameters were obtained. Linear correlations between X_c and DSC crystallization parameter e.g., S_i, ΔW, A/m and ΔH are shown in Table III, with R^2 values 0.80, 0.75, 0.71, and 0.86, respectively.

The following observations may be made from the correlations shown in Table III. In the HDPE/TWF composites, the breaking elongation is dependent on the crystallinity and nucleation rate. The impact strength is also governed by the crystallinity. These imply the important role of crystallinity of HDPE in the tensile and impact properties of the composites.

In the HDPE/TWF/HDPE-g-MAH composites, the coupling agent modifies the correlations appreciably. The general trends of the correlation curves remain similar as in the HDPE/TWF composites, the slopes and intercepts of the curves change in some of the correlations. Thus, S_i and ΔH did not show linear correlations with tensile modulus in the HDPE/TWF systems, the parameters presented linear correlations in presence of the coupling agent. Similarly, linear correlations were not observed for ΔW and A/m vs. ε (%), S_i and ΔW vs. I, and S_i, ΔW, and A/m vs. X_c in the HDPE/TWF composites whereas all these pair of variables exhibited linear correlations in the HDPE/TWF/HDPE-g-MAH systems. It may be emphasized that for those pairs of variables, which registered lower R^2 values, the correlations could be more complex than the linear equations.

The results indicate that in the HDPE/TWF composites tensile modulus, strength, elongation-at-break, and impact strength decrease with decreasing crystallinity, because filler imposes mechanical restraint and creates weak interphase. In presence of the coupling agent, the modulus and tensile strength increase despite decrease in crystallinity due to enhanced phase interaction. However, the ductility of the systems decreases as in the HDPE/TWF composites.

CONCLUSIONS

The crystallization and melting properties of HDPE in the HDPE/TWF and the HDPE/TWF/HDPE-g-MAH composites have been evaluated by DSC and X-ray studies. The crystallinity data by the two methods are supportive to each other.

The TWF decreases the crystallinity of HDPE through mechanical restraints. However, the interphase becomes quite weak so that the tensile strength, modulus, breaking elongation, and impact strength decrease. In presence of the coupling agent, HDPE-g-MAH, the interphase becomes stronger which decreases the crystallinity. However, tensile strength and modulus enhanced due to predominant effect of phase interaction due to the physical interaction and chemical bonding between HDPE and TWF particles. The ductility does not change in the

presence of coupling agent and thus the breaking elongation and impact strength decreases.

Authors are thankful to the Senior Research Fellowship to one of them (Kamini Sewda).

References

1. Li, Q.; Matuana, L. M. J Thermoplast Compos Mater 2003, 16, 551.
2. Maiti, S. N.; Hassan, M. R. J Appl Polym Sci 1989, 37, 2019.
3. Li, Q.; Matuana, L. M. J Appl Polym Sci 2003, 88, 278.
4. Rizvi, G.; Matuana, L. M.; Park, C. B. Polym Eng Sci 2000, 40, 2124.
5. Brydson, J. A. Plastics Materials; Butterworth Heinemann: New York, 1999.
6. Maiti, S. N.; Sharma, K. K. J Mater Sci 1992, 27, 4605.
7. Sewda, K.; Maiti, S. N. J Appl Polym Sci 2007, 105, 2598.
8. Maiti, S. N.; Singh, K. J Appl Polym Sci 1986, 32, 4285.
9. Sewda, K.; Maiti, S. N. J Appl Polym Sci 2009, 112, 1826.
10. Stark, N. M.; Matuana, L. M. J Appl Polym Sci 2003, 90, 2609.
11. Stark, N. M.; Matuana, L. M. Polym Degrad Stab 2004, 86, 1.
12. Bledzki, A. K.; Gassan, J. Prog Polym Sci 1999, 24, 221.
13. Bledzki, A. K.; Gassan, J.; Theis, S. Mechan Compos Mater 1998, 34, 563.
14. Clemons, C. M.; Ibach, R. E. Forest Prod J 2004, 54, 50.
15. Khonakdar, H. A.; Jafari, S. H.; Taheri, M.; Wagenknecht, U.; Jehnichen, D.; Haüssler, L. J Appl Polym Sci 2006, 100, 3264.
16. David, D. J.; Mishra, A. Relating Materials Properties to Structure: Handbook and Software for Polymer Calculations and Material Properties; Technomic Publishing Co., Inc.: Lancaster, Basel, 1999.
17. Zheng, Q.; Peng, M.; Yi, X. Mater Lett 1999, 40, 91.
18. Feng, Y.; Jin, X.; Hay, J. N. J Appl Polym Sci 1998, 69, 2469.
19. Campbell, D.; Qayyum, M. M. J Polym Sci Polym Phys 1980, 18, 83.
20. Pukanszky, B.; Belina, K.; Rockenbauer, A.; Maurer, F. H. J. Composites 1994, 25, 205.
21. Leong, Y. W.; Abu Bakar, M. B.; Ishak, Z. A. M.; Ariffin, A. J Appl Polym Sci 2005, 98, 413.
22. Rodriguez, F. Principles of Polymer Systems; Taylor & Francis: Washington, DC, 1996.
23. Painter, P. C.; Coleman, M. M. Fundamentals of Polymer Science: An Introductory Text; Technomic Publishing Company, Inc.: Lancaster, Pennysylvania, 1994.
24. Ehrenstein, G. W.; Riedel, G.; Pia, T. Thermal Analysis of Polymers; Carl Hancer Verlag: Munich, 2004.
25. Maiti, S. N.; Mahapatro, P. K. J Appl Polym Sci 1989, 37, 1889.
26. Gupta, A. K.; Purwar, S. M. J Appl Polym Sci 1984, 22, 3513.
27. Product Literature, GAIL. Available at: http://www.gailonline.com/petrochemicals/i58a180.htm (accessed May 2005).
28. Pluss Polymers, F-213/B, 1st Floor, Lado Sarai, New Delhi-110030, India. Available at: www.plusspolymers.com (accessed May 2005).
29. Wood-Plastic Composites. TechLine, Forest Product Laboratory, Issued 01/04.
30. Gupta, A. K.; Gupta, V. B.; Peters, R. H.; Harland, W. G.; Berry, J. P. J Appl Polym Sci 1982, 27, 4669.
31. Maiti, S. N.; Ghosh, K. J Appl Polym Sci 1994, 52, 1091.
32. Beck, H. N. J Appl Polym Sci 1967, 11, 673.
33. Gupta, A. K.; Ratnam, B. K. J Appl Polym Sci 1991, 42, 297.
34. Brandrup, J.; Immergut, E. H. Polymer Handbook; John Wiley and Sons: New York, 1989.
35. Annual Book of ASTM Standard, Part 37; ASTM: Philadelphia, 1976.
36. Joshi, M.; Misra, A.; Maiti, S. N. J Appl Polym Sci 1991, 43, 311.
37. Jose, S.; Aprem, A. S.; Francis, B.; Chandy, M. C.; Werner, P.; Alstaedt, V.; Thomas, S. Eur Polym J 2004, 40, 2105.
38. Zhu, Y.; Chang, L.; Yu, S. J Therm Anal 1995, 45, 329.
39. Fillon, B.; Thierry, A.; Lotz, B.; Wittmann, J. C. J Therm Anal Calor 1994, 42, 721.
40. Stark, N. M.; Matuana, L. M. Polym Degrad Stab 2007, 92, 1883.
41. Gray, D. G. J Polym Sci Polym Lett Ed 1974, 12, 645.
42. Baker, W. E.; Windle, A. H. Polymer 2001, 42, 667.
43. Guan, Q.; Lai, F. S.; Mccarthy, S. P.; Chiu, D.; Zhu, X.; Shen, K. Polymer 1997, 38, 5251.
44. Beck, H. N.; Ledbetter, H. D. J Appl Polym Sci 1965, 9, 2131.